UCRL-ID-119565 Rev. 1

Calculation of a Residual Mean Meridional Circulation for a Zonal-Mean Transport Model

·Woo Kap Choi, †Douglas A. Rotman, *Donald J. Wuebbles

†Lawrence Livermore National Laboratory
7000 East Avenue, L-262
Livermore, California 94550

and

*University of Illinois
Department of Atmospheric Sciences
105 S. Gregory Avenue
Urbana, Illinois 61801

January 1995

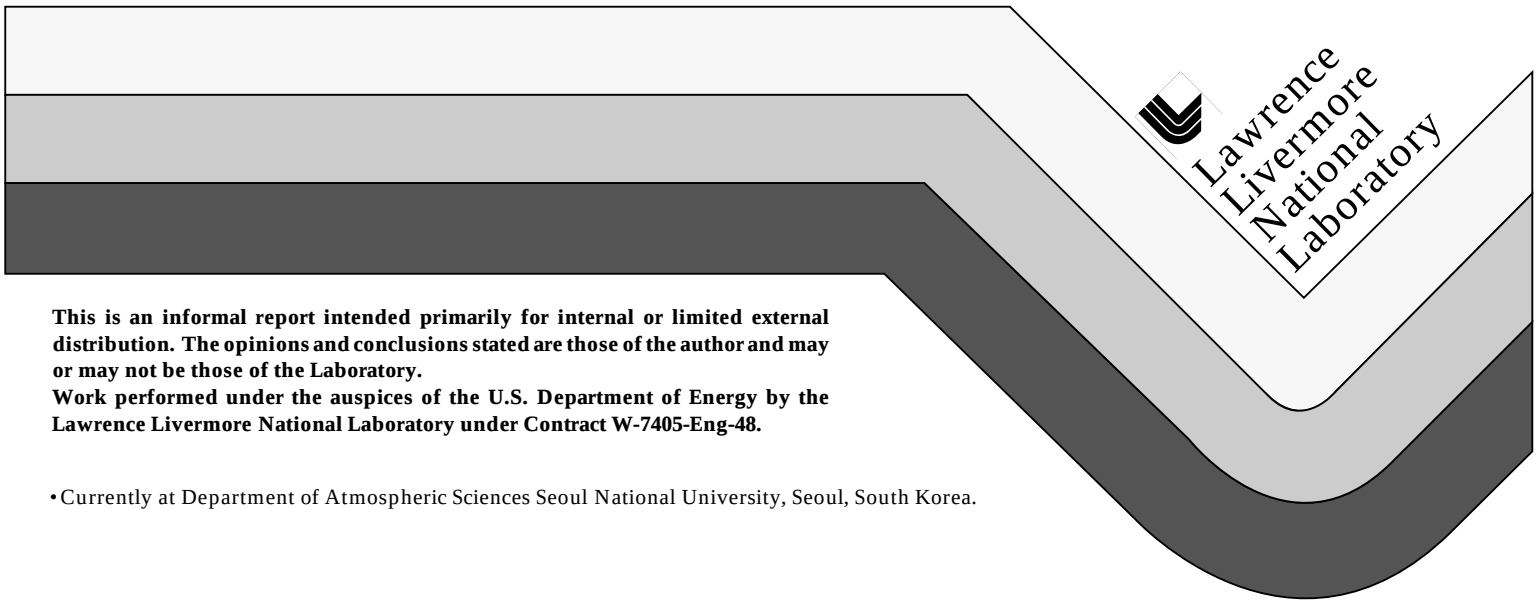

Work performed under the auspices of the U.S. Department of Energy by the Lawrence Livermore National Laboratory under Contract W-7405-Eng-48.

• Currently at Department of Atmospheric Sciences Seoul National University, Seoul, South Korea.

Calculation of a Residual Mean Meridional Circulation for a Zonal-Mean Tracer Transport Model

W. K. Choi, D. A. Rotman and D. J. Wuebbles

Global Climate Research Division
Lawrence Livermore National Laboratory

1. Introduction

Because of their computational advantages, zonally-averaged chemical-radiative-transport models are widely used to investigate the distribution of chemical species and their change due to the anthropogenic chemicals in the lower and middle atmosphere. In general, the Lagrangian-mean formulation would be ideal to treat transport due to the zonal mean circulation and eddies. However, the Lagrangian formulation is difficult to use in practical applications (McIntyre, 1980). The most widely-used formulation for treating global atmospheric dynamics in two-dimensional models is the transformed Eulerian mean (TEM) equations (Andrews and McIntyre, 1976). The residual mean meridional circulation (RMMC) in the TEM system is used to advect tracers. In this study, we describe possible solution techniques for obtaining the RMMC in the LLNL two-dimensional chemical-radiative-transport model. In the next section, the formulation will be described. In sections 3 and 4, possible solution procedures will be described for a diagnostic and prognostic case, respectively.

2. Formulation

The set of equations in the TEM formulation are given as

$$\frac{\partial \overline{u}}{\partial t} - \overline{v}^* \left[f - \frac{1}{\cos\phi} \frac{\partial}{\partial y} \left(\overline{u} \cos\phi \right) \right] + \overline{w}^* \frac{\partial \overline{u}}{\partial z} = \frac{1}{\rho_0} \nabla \cdot \mathbf{F} \tag{1}$$

$$\left(f + \frac{2 \tan\phi}{a} \right) \frac{\partial \overline{u}}{\partial z} = \frac{R}{H} e^{-\kappa z / H} \frac{\partial \overline{\theta}}{\partial y} \tag{2}$$

$$\frac{\partial \overline{\theta}}{\partial t} + \overline{v}^* \frac{\partial \overline{\theta}}{\partial y} + \overline{w}^* \frac{\partial \overline{\theta}}{\partial z} = \overline{Q} + \overline{E} \tag{3}$$

$$\frac{1}{\rho_0} \frac{\partial}{\partial y} \left(\cos\phi \, \overline{v}^* \right) + \frac{1}{\cos\phi} \frac{\partial}{\partial z} \left(\rho_0 \, \overline{w}^* \right) = 0 \tag{4}$$

$$\frac{\partial \overline{\mu}}{\partial t} + \overline{v}^* \frac{\partial \overline{\mu}}{\partial y} + \overline{w}^* \frac{\partial \overline{\mu}}{\partial z} = \overline{S} + \frac{1}{\cos\phi} \frac{\partial}{\partial y} \left(\cos\phi \, K_{yy} \frac{\partial \overline{\mu}}{\partial y} \right) + \frac{1}{\rho_0} \frac{\partial}{\partial z} \left(\rho_0 \, K_{zz} \frac{\partial \overline{\mu}}{\partial z} \right) \tag{5}$$

where $\overline{E}$ is the eddy heat flux convergence and μ is the mixing ratio of chemical species. The other notations have their usual meanings (see, for example, Andrews et al., 1987). The RMMC obtained from the first four equations is used to advect chemical tracers in (5).

The first four equations constitute a closed set of equations including two prognostic equations and two diagnostic equations with four unknown variables. The solution procedures are dependent on treatment of the temporal variations of the zonal wind and temperature. If the temporal variation of the temperature is negligible or can be specified, then the system becomes diagnostic and it is easier to solve for the circulation as only two equations are needed (see description in the next section). A disadvantage of this diagnostic system is that the radiative and

photochemical feedback on the dynamics is neglected. To handle this feedback, temperature and zonal wind should be treated as prognostic values. In this prognostic system, temperature and zonal wind are calculated as well as the RMMC, using all four equations (1) to (4).

3. Diagnostic system

If the temporal variations of zonal wind and temperature are ignored or known, only two equations, including (4) and either (1) or (3), are needed to solve for the RMMC. Choosing which equation between (1) or (3) depends on the difficulty of estimating the Eliassen-Palm (EP) flux divergence, $\nabla \cdot \mathbf{F}$, and the diabatic heating rate, $\overline{Q}$. For two-dimensional models, the thermodynamic energy equation is generally used as the EP flux divergence is not computed in those models. Calculating the RMMC from the zonal momentum equation is useful for certain studies, for example, recently, Rosenlof and Holton (1993) obtained the residual circulation they calculated based on the EP flux divergence from the observed data.

The solution procedure for the diagnostic equation system is easier than that of prognostic system, but there are some special difficulties to resolve. As noted by Tung (1982), the two variables of interest, $\overline{v}^*$ and $\overline{w}^*$, require two equations for solution; and furthermore, there is a constraint that must be satisfied. The constraint is given as

$$\int_{-\pi/2}^{\pi/2} \cos\phi \, \overline{w}^* \, d\phi = 0 \qquad (6a)$$

or

$$\int_{-\pi/2}^{\pi/2} \left(\overline{Q} + \overline{E} - \frac{\partial \overline{\theta}}{\partial t} - \overline{v}^* \frac{\partial \overline{\theta}}{\partial y} \right) \frac{\cos\phi}{\partial \overline{\theta} / \partial z} \, d\phi = 0 \qquad (6b)$$

The problem is that the meridional velocity in the integrand is itself unknown. The physically correct way of adjusting heating rates is using heating rates on isentropic surfaces (Yang et al., 1990; Choi and Holton, 1991) on which the meridional advection of heat vanishes. This isentropic adjustment of heating rates is discussed in Appendix A. However, in the most two-dimensional models, isobaric coordinates are used and interpolation of heating rates onto isentropic surface is not very simple. For the isobaric system, Shine (1989) discussed several methods of satisfying the above constraint. The most popular way is subtracting the global average of the vertical velocity from velocities at each grid point on isobaric surfaces. In this case the heating rates given originally is not changed before and after calculation. Some scientists (e.g., Rosenfield et al., 1987) adjust the heating rates for the global average heating to vanish before calculation of the circulation. As shown in the Appendix B, this procedure makes the global average of the vertical circulation multiplied by potential temperature vanish and could be a good approximation of (6a) in the middle atmosphere.

Below, we provide two methods for the solution of the diagnostic equation set.

a. Successive substitution

The vertical velocity in (3) can be rewritten by

$$\overline{w}^* = \left(\overline{Q} + \overline{E} - \frac{\partial \overline{\theta}}{\partial t} - \overline{v}^* \frac{\partial \overline{\theta}}{\partial y} \right) / \frac{\partial \overline{\theta}}{\partial z} \qquad (7)$$

The first step is assuming the zero meridional velocity. The vertical velocity can then be obtained directly and can be used to obtain the meridional velocity through the continuity equation. This is the procedure used by Dunkerton (1978) for the winter solstice condition. To include the effect of the meridional advection, the meridional velocity is then substituted to obtain the vertical velocity. This procedure continues until the solution converges. The vertical velocity should be modified at each time step to satisfy the constraint (6a). Examples of vertical and meridional velocities calculated from the total heating rates given in Fig. 1 from the LLNL 2-D model are shown in Figs. 2 and 3.

An assumption in this method is that the meridional advection of heat is much smaller than the vertical advection. This assumption is true in the middle atmosphere where the slopes of isentropic surfaces are not steep. In the troposphere, however, it is not always applicable. This method of successive substitution does not always converge. Even though the solution converges, the number of iterations in the model domain including the troposphere is much bigger than that of the region including the middle atmosphere only.

If we knew whether the iteration would succeed or fail before calculation, it would be very convenient. There is a convergence criteria of the successive substitution method for simple nonlinear equations (for example, see Pearson, 1986). We are not aware if there is a similar criteria in this case.

b. Using an advection equation

When the method of successive substitution does not yield a converging solution, a new technique is required. Instead of solving the two equations simultaneously, one equation can be constructed from two equations utilizing the stream function and can then be solved. An example of similar technique is found in Holton and Choi (1988). A discussion about the stream function is found in Appendix C.

Here we define the stream function ψ by

$$\rho_0 \cos\phi \, \overline{v}^* = -\frac{\partial \psi}{\partial z} \tag{8a}$$

$$\rho_0 \cos\phi \, \overline{w}^* = \frac{\partial \psi}{\partial y} \tag{8b}$$

then the thermodynamic energy equation becomes an advection equation of the stream function

$$\frac{\partial \psi}{\partial y} + \overline{S} \frac{\partial \psi}{\partial z} = \tilde{Q} \tag{9a}$$

where the isentropic slope $\overline{S}$ and heating $\tilde{Q}$ is defined by

$$\overline{S} = -\frac{\partial \overline{\theta}}{\partial y} / \frac{\partial \overline{\theta}}{\partial z} \tag{9b}$$

$$\tilde{Q} = \rho_0 \cos\phi \left(\overline{Q} + \overline{E} - \frac{\partial \overline{\theta}}{\partial t} \right) / \frac{\partial \overline{\theta}}{\partial z} \tag{9c}$$

The numerical scheme we chose to solve (9) is the trapezoidal implicit scheme (Haltiner and Williams, 1980). This scheme is numerically stable. A disadvantage of this implicit scheme is that we have to invert a matrix to get a solution. However, the matrix is tridiagonal and therefore can be easily solved by the tridiagonal algorithm (see, for example,

Richtmyer and Morton, 1967, Roache, 1972). A more serious problem in this scheme is that we cannot choose the direction of integration freely. The factor determining the direction is the magnitude of the grid intervals and $\overline{S}$. The possible direction of integration is meridional one in this case. In meridional integration the boundary condition at the top of the model domain is required. For this top boundary condition, the stream function is obtained using (8b) from the vertical velocity in Fig. 2. This stream function (Fig. 4) can be compared with the results from those calculated by the trapezoidal implicit scheme.

To calculate the RMMC from the heating rate in Fig. 1, adjustment of heating rate prior to the calculation is required since the solution technique does not have a procedure satisfying the constraint (6a). In this study, we applied the zero net heating condition although it is not always satisfactory in the troposphere.

The solution procedure takes three steps. The first step is an integration from the South pole to the North pole by using the zero surface value and prescribed value at the top. The result from this step is shown in Fig. 5a. In an ideal case, the values of stream function would turn out to be exactly zero at the North pole. While the stream function is close to zero in the middle atmosphere at the North pole, it is different from zero in the troposphere. In the second step, the integration takes from the North pole to the South pole (Fig. 5b). And in the third step, constructing a set of stream function out of two by using Southern Hemispheric value from Fig. 5a and Northern Hemispheric value from Fig. 5b. At the equator, the stream function should be matched. The result is shown in Fig. 5c. The justification of this method lies in the fact that the heating rates is not so accurate as boundary conditions in this problem. The boundary conditions

are more accurate and valuable than heating rates and therefore we have to utilize this fact.

4. Prognostic system

The four equations from (1) to (4) can be combined into an equation for stream function following Garcia and Solomon (1983). The temporal variation of the zonal wind and temperature can be removed through the thermal wind equation if the tangent factor of the relationship is neglected. The stream function χ is defined by

$$\rho_0 \cos\phi \, \overline{v}^* = -\frac{\partial}{\partial z}(\rho_0 \chi) \tag{10a}$$

$$\rho_0 \cos\phi \, \overline{w}^* = \frac{\partial}{\partial y}(\rho_0 \chi) \tag{10b}$$

The combined equation for χ is as follows:

$$C_{yy}\chi_{yy} + C_{yz}\chi_{yz} + C_{zz}\chi_{zz} + C_y\chi_y + C_z\chi_z + C\chi = C_f \tag{11}$$

where the coefficients are

$$C_{yy} = \frac{R}{H} e^{-\kappa z / H} \frac{\partial \overline{\theta}}{\partial z} \tag{12a}$$

$$C_{yz} = 2f \frac{\partial \overline{u}}{\partial z} \tag{12b}$$

$$C_{zz} = f\left(f - \frac{\partial \overline{u}}{\partial y} + \frac{\overline{u} \tan\phi}{a} \right) \tag{12c}$$

$$C_y = \frac{R}{H} e^{-\kappa z / H} \frac{\partial \overline{\theta}}{\partial z} \frac{\tan\phi}{a} - (1+\kappa)\frac{f}{H}\frac{\partial \overline{u}}{\partial z} \tag{12d}$$

$$C_z = -\frac{f}{H}\left(f - \frac{\partial \overline{u}}{\partial y} + \frac{\overline{u}\tan\phi}{a}\right) + \left(\frac{2f\tan\phi}{a} + \frac{df}{dy}\right)\frac{\partial \overline{u}}{\partial z} \qquad (12e)$$

$$C = -\frac{1}{H}\left(\frac{2f\tan\phi}{a} + \frac{df}{dy}\right)\frac{\partial \overline{u}}{\partial z} \qquad (12f)$$

$$C_f = \cos\phi\left[f\frac{\partial}{\partial z}\left(\frac{1}{\rho_0}\nabla\cdot\mathbf{F}\right) + \frac{R}{H}e^{-\kappa z/H}\frac{\partial}{\partial y}(Q+E)\right] \qquad (12g)$$

Among the above coefficients, C_{yy} and C_y ,are slightly different from what are given by Garcia and Solomon (1983) who used the temperature instead of potential temperature in the thermodynamic energy equation. Also the last term in the left hand side is not neglected. Contrast to the diagnostic system, the knowledge of both EP flux divergence and the total diabatic heating is required to solve (11). At the side boundary, the stream function can be set to be zero. The bottom boundary condition is either specified (Brasseur et al., 1990) or is calculated through the "downward control principle" (Holton, 1990; Haynes et al., 1991; Garcia, 1991; Rosenlof and Holton, 1993). At the top $\partial\chi/\partial z = 0$ is usually specified.

In the LLNL two-dimensional model, one solution for (11) is obtained by the method suggested by Lindzen and Kuo (1969). The numerical scheme is described in Choi and Wuebbles (1993) in detail.

To test the solution technique we need the thermal and momentum forcing. In the first step, we obtain the meridional circulation by the successive substitution from the given heating rates (Fig. 6) with assuming zero temporal variability of wind and temperature. The vertical and meridional velocities obtained this way (Figs. 7 and 8) and the zonal wind and temperature are used to construct the EP flux divergence and heating

rates through (1) and (3) respectively. The heating rates and the zonal momentum forcing (EP flux divergence divided by density) constructed are shown in Figs. 9 and 10. These values can then be used as forcing terms in (11). The stream function solved with zero bottom boundary condition is shown in Fig. 11 and the vertical and meridional velocities obtained from this stream function are shown in Figs. 12 and 13.

In an ideal case, the meridional circulations before (Figs. 7, 8) and after (Figs. 12, 13) the calculation of (11) should be identical. There are, however, some differences between those two sets of circulation. There are several reasons for these differences. In the elliptic solver for (11) we have to assume the top boundary condition; the choice of boundary condition may not resemble real features. Another reason is that we ignored the tangent factor, which is the second term in the left hand side of the thermodynamic equation (2) when we construct the equation (11). The numerical error in the different finite difference forms might also play a role. The pattern in Figs. 12 and 13 are much smoother than that of Figs. 7 and 8 due to the smoothing effect of the elliptic solver.

Acknowledgments The authors are grateful to Drs. Karl Taylor, Keith Grant and Jinwon Kim for helpful discussions. This work was performed under the auspices of the U. S. Department of Energy by the Lawrence Livermore National Laboratory under contract No. W-7405-Eng-48 and was supported in part by the Department of Energy's Carbon Dioxide Research Program and by the NASA's Atmospheric Chemistry Modeling and Analysis Program.

APPENDIX A

Zero Net Heating on Isentropic Surface

We are going to show that the global average of the density-weighted net heating rates on an isentropic surface is close to zero. From the continuity equation for the isentropic coordinates, (for example, Andrews et al., 1987)

$$\frac{\partial \sigma}{\sigma t} + \frac{\partial}{\partial x}(\sigma u) + \frac{1}{\cos}\frac{\partial}{\partial y}(\sigma v \cos\phi) + \frac{\partial}{\partial \theta}(\sigma Q) = 0 \qquad \text{(A1)}$$

where Q is the diabatic heating rate and σ is the density in the isentropic coordinates defined by

$$\sigma \equiv -\frac{1}{g}\frac{\partial p}{\partial \theta} \qquad \text{(A2)}$$

Zonal averaging of (A1) on isentropic surfaces gives

$$\frac{\partial \overline{\sigma}}{\partial t} + \frac{1}{\cos\phi}\frac{\partial}{\partial y}\left(\overline{\sigma v}\cos\phi\right) + \frac{\partial}{\partial \theta}\left(\overline{\sigma Q}\right) = 0 \qquad \text{(A3)}$$

Using the definition of σ, we can rewrite (A3) as

$$\frac{\partial}{\partial \theta}\left(-\frac{1}{g}\frac{\partial \overline{p}}{\partial t} + \overline{\sigma Q}\right) + \frac{1}{\cos\phi}\frac{\partial}{\partial y}\left(\overline{\sigma v}\cos\phi\right) = 0 \qquad \text{(A4)}$$

Multiplying $\cos\phi$ and integrating (A4) in latitudes from South pole to North pole eliminates the second term in (A4) and yields

$$\int_{-\pi/2}^{\pi/2} \cos\phi \frac{\partial}{\partial\theta}\left(-\frac{1}{g}\frac{\partial\overline{p}}{\partial t}+\overline{\sigma Q}\right) a\,d\phi = 0 \qquad \text{(A5)}$$

Integrating (A5) in altitude from the top of the atmosphere to θ^* gives

$$\int_{-\pi/2}^{\pi/2} \cos\phi \left[-\frac{1}{g}\frac{\partial\overline{p}}{\partial t}+\overline{\sigma Q}\right]_{\theta^*} a\,d\phi = 0 \qquad \text{(A6)}$$

since $p = \sigma = 0$ at the top of the atmosphere. θ^* is an arbitrary potential temperature whose surface does not meet the ground. Rearranging the terms of (A6) gives

$$\int_{-\pi/2}^{\pi/2} \overline{\sigma Q} \cos\phi d\phi = \frac{d}{dt}\int_{-\pi/2}^{\pi/2} \frac{\overline{p}}{g}\cos\phi d\phi \qquad \text{(A7)}$$

Equation (A7) can be rewritten as

$$\int_{-\pi/2}^{\pi/2} \overline{\sigma Q} \cos\phi d\phi = \frac{1}{2\pi a^2}\frac{dM^*}{dt} \qquad \text{(A8)}$$

where M^* is total mass between the isentrope θ^* and the top of the atmosphere defined by

$$M^* \equiv \int_{-\pi/2}^{\pi/2}\int_{0}^{2\pi} \frac{p}{g} a^2 \cos\phi d\lambda d\phi = \frac{2\pi a}{g}\int_{-\pi/2}^{\pi/2} \overline{p}\cos\phi a\,d\phi \qquad \text{(A9)}$$

Since dM^*/dt is negligible (A8) becomes

$$\int_{-\pi/2}^{\pi/2} \overline{\sigma Q} \cos\phi d\phi \approx 0 \qquad \text{(A10)}$$

and thus we showed that the global average of the density-weighted heating is negligible.

In the zonally-averaged formulation, (A10) cannot be used since the relationship between the density and the heating rate is unknown following the latitude circle. If we assume the covariance of the perturbations $\overline{\sigma' Q'}$ to be negligible, then (A10) is rewritten as

$$\int_{-\pi/2}^{\pi/2} \bar{\sigma}\overline{Q} \cos\phi d\phi \approx 0 \qquad \text{(A11)}$$

which is a practical form for the heating rates adjustment in the zonal mean model. In the middle atmosphere (A11) can be further simplified to give

$$\int_{-\pi/2}^{\pi/2} \overline{Q} \cos\phi d\phi \approx 0 \qquad \text{(A12)}$$

since the slope of the isentropic surface on the isobaric coordinates are very small and thus the density does not change much on an isentrope.

APPENDIX B

Zero Net Heating on Isobaric Surface

The flux form of the thermodynamic energy equation (3) can be written by

$$\frac{\partial}{\partial y}\left(\rho_0 \cos\phi \,\overline{v}^* \overline{\theta}\right) + \frac{\partial}{\partial z}\left(\rho_0 \cos\phi \,\overline{w}^* \overline{\theta}\right) = \rho_0 \cos\phi \left(\overline{Q} + \overline{E} - \frac{\partial \overline{\theta}}{\partial t}\right) \qquad \text{(B1)}$$

Integration of the above equation in latitude from South pole to North pole eliminates the first term in the left hand side and thus

$$\int_{-\pi/2}^{\pi/2} \frac{\partial}{\partial z}\left(\rho_0 \cos\phi\, \overline{w}^{*}\overline{\theta}\right) d\phi = \rho_0 \int_{-\pi/2}^{\pi/2} \cos\phi \left(\overline{Q} + \overline{E} - \frac{\partial \overline{\theta}}{\partial t} \right) d\phi \qquad \text{(B2)}$$

The right hand side of (B2) is the net heating rates on an isobaric surface. If we set this value be zero and integrate (B2) from z to infinity in altitude, then we get

$$\int_{-\pi/2}^{\pi/2} \cos\phi\, \overline{w}^{*}\overline{\theta}\, d\phi = 0 \qquad \text{(B3)}$$

Therefore putting the net heating rates to be zero is consistent with putting the global average of the vertical velocity multiplied by potential temperature to be zero. If the potential temperature does not change significantly on isobaric surfaces, then (B3) could be a close approximation of (6a).

APPENDIX C

Stream Functions

The continuity equation (4) can be rewritten as

$$\frac{\partial}{\partial y}\left(\rho_0 \cos\phi\, \overline{v}^{*}\right) + \frac{\partial}{\partial z}\left(\rho_0 \cos\phi\, \overline{w}^{*}\right) = 0 \qquad \text{(C1)}$$

Stream functions satisfying the above equation can be defined in many ways. We are going to discuss three types of stream functions found in literature. They are ψ_1, ψ_2 and ψ_3 defined by

$$\rho_0 \cos\phi\ \overline{v}^* = -\frac{\partial \psi_1}{\partial z} = -\frac{\partial}{\partial z}\left(\rho_0 \psi_2\right) = -\frac{\partial}{\partial z}\left(\cos\phi\ \psi_3\right) \qquad \text{(C2a)}$$

$$\rho_0 \cos\phi\ \overline{w}^* = \frac{\partial \psi_1}{\partial y} = \frac{\partial}{\partial y}\left(\rho_0 \psi_2\right) = \frac{\partial}{\partial y}\left(\cos\phi\ \psi_3\right) \qquad \text{(C2b)}$$

The widely used stream functions are ψ_1 and ψ_2. We are going to concentrate on these and postpone the discussion about ψ_3 later.

ψ_1 is the mass flux stream function and identical to ψ in the Section 3b. It is found in some papers (e.g., Hitchman and Leovy, 1986, Holton and Choi, 1988). Since ψ_1 is presenting the real path of mass, it is useful for diagnostic purpose (see Figs. 4 and 5). ψ_2 is identical to χ in the Section 4 and is also found in many papers (Garcia and Solomon, 1983; Solomon et al., 1986; Brasseur et al., 1990, Garcia et al., 1992). Brasseur et al. (1990) called ψ_2 as the "velocity" stream function contrast to the "mass" stream function of ψ_1. There is an advantage in using ψ_2 instead of ψ_1. Since ψ_2 does not include the density factor, its variation is close to linear (see Fig. 11) and thus it is easier to specify the top boundary condition in terms of ψ_2.

To use stream functions we need appropriate boundary conditions. If we assume $\overline{w}^*$ to be zero at the surface and use the fact that $\overline{v}^*$ is zero at the both poles, then the boundary conditions for ψ_1 will be

$$\psi_1 = 0 \qquad \text{at} \qquad z = 0 \qquad \text{(C3a)}$$

$$\psi_1 = 0 \qquad \text{at} \qquad \phi = \pm\pi/2 \qquad \text{(C3b)}$$

without loss of generality. The same boundary conditions can be applied to ψ_2 as well. The above conditions, however, would be sufficient but not necessary conditions for ψ_2. The general boundary conditions for ψ_2 are

$$\psi_2 = c \qquad \text{at} \qquad z = 0 \tag{C4a}$$

$$\psi_2 = ce^{z/H} \qquad \text{at} \qquad \phi = \pm\pi/2 \tag{C4b}$$

where c is an arbitrary constant. If we have an additional condition, $\partial\psi_2 / \partial z = 0$ at the top of the domain, which is not an unreasonable approximation, then c should be zero.

Among many types of stream functions only one function satisfies the "conventional" definition which is that the streamlines are parallel to the velocity field. To test the above point we take the differential of ψ_1

$$d\psi_1 = \frac{\partial\psi_1}{\partial y}\,dy + \frac{\partial\psi_2}{\partial z}\,dz \tag{C5}$$

which can be rewritten, using (C2), as

$$d\psi_1 = \left(\rho_0 \cos\phi\, \overline{w}^*\right)dy + \left(\rho_0 \cos\phi\, \overline{v}^*\right)dz \tag{C6}$$

On the streamline we have a condition of $d\psi_1 = 0$ and thus we get

$$\left(\frac{dz}{dy}\right)_{\psi_1=\text{const}} = \frac{\overline{w}^*}{\overline{v}^*} \tag{C7}$$

which is a condition of the streamline of ψ_1 is parallel to the velocity field $\left(\overline{v}^*, \overline{w}^*\right)$. Likewise we can test ψ_2 by the same method, which gives us

$$\left(\frac{dz}{dy}\right)_{\psi_2=\text{const}} = -\frac{\partial\psi_2/\partial y}{\partial\psi_2/\partial z} = \frac{\cos\phi\,\overline{w}^*}{\cos\phi\,\overline{v}^* - \frac{\psi_2}{H}} \tag{C8}$$

which becomes identical to (C7) only when $\psi_2 = 0$.

The third stream function ψ_3 is identical to $\overline{\chi}^*_{\text{mass}}$ used in Garcia and Solomon (1983) and Solomon et al. (1986). Garcia and Solomon (1983) noted that "isopleths of $\overline{\chi}^*_{\text{mass}}$ coincide with the streamlines of the velocity field in the meridional plane". The above statement, however, is not true. On the constant ψ_3 line we get

$$\left(\frac{dz}{dy}\right)_{\psi_3=\text{const}} = -\frac{\partial\psi_3/\partial y}{\partial\psi_3/\partial z} = \frac{\rho_0\overline{w}^* + \frac{\psi_3\tan\phi}{a}}{\rho_0\overline{v}^*} \tag{C9}$$

ψ_3 coincides with the velocity field only at the both poles ($\psi_3 = 0$) and on the equator ($\tan\phi = 0$) exactly. However, ψ_3 may look similar to ψ_1 in the most region of the atmosphere (see Fig. 2 by Solomon et al., 1986).

The two equations in p.1387 in Garcia and Solomon (1983) are incorrect. They should be read

$$\overline{\chi}^*_{\text{mass}} = \rho_s\overline{\chi}^* \tag{C10}$$

$$\left(\overline{v}^*, \overline{w}^*\right) = \mathbf{i}\times\frac{1}{\rho_s\cos\theta}\nabla\overline{\chi}^*_{\text{mass}} \tag{C11}$$

where they used notations ρ_s and θ instead of our ρ_0 and ϕ. The definition of the "mass weighted stream function" in Solomon et al. (1986) should also be corrected following (C10).

REFERENCES

Andrews, D. G., and M. E. McIntyre, 1976: Planetary waves in horizontal and vertical shear: The generalized Eliassen-Palm relation and the mean zonal acceleration. *J. Atmos. Sci.*, **33**, 2031-2048.

Andrews, D. G., J. R. Holton, and C. B. Leovy, 1987: *Middle Atmosphere Dynamics*, Academic Press, New York, 489 pp.

Brasseur, G., M. H. Hitchman, S. Walters, M. Dymek, E. Falise, and M. Pirre, 1990: An interactive chemical dynamical radiative two-dimensional model of the middle atmosphere. *J. Geophys. Res.*, **95**, 5639-5655.

Choi, W. K., and J. R. Holton, 1991: Transport of N_2O in the stratosphere related to the equatorial semiannual oscillation. *J. Geophys. Res.*, **96**, 22,543-22,557.

Choi, W. K., and D. J. Wuebbles, 1993; *Numerical procedure for a parameterization of the planetary wave breaking*. Lawrence Livermore National Laboratory, UCRL-pending.

Dunkerton, T., 1978: On the mean meridional mass motions of the stratosphere and mesosphere. *J. Atmos. Sci.*, **35**, 2325-2333.

Garcia, R. R., 1991: Parameterization of planetary wave breaking in the middle atmosphere. *J. Atmos. Sci.*, **48**, 1405-1419.

Garcia, R. R., and S. Solomon, 1983: A numerical model of the zonally averaged dynamical and chemical structure of the middle atmosphere. *J. Geophys. Res.*, **88**, 1379-1400.

Garcia, R. R., F. Stordal, S. Solomon, and J. T. Kiehl, 1992: A new numerical model of the middle atmosphere, 1, Dynamics and transport of tropospheric source gases. *J. Geophys. Res.*, **97**, 12,967-12,991.

Haltiner, G. J., and R. T. Williams, 1980: *Numerical Prediction and Dynamic Meteorology* 2nd ed., John Wiley & Sons, 477pp.

Haynes, P. H., C. J. Marks, M. E. McIntyre, T. G. Shepherd, and K. P. Shine, 1991: On the "downward control" of extratropical diabatic circulations by eddy-induced mean zonal forces. *J. Atmos. Sci.*, **48**, 651-678.

Hitchman, M. H., and C. B. Leovy, 1986: Evolution of the zonal mean state in the equatorial middle atmosphere during October 1978-May 1979. *J. Atmos. Sci.*, **43**, 3159-3176.

Holton, J. R., 1990: On the global exchange of mass between the stratosphere and troposphere. *J. Atmos. Sci.*, **47**, 392-395.

Holton, J. R., and W. K. Choi, 1988: Transport circulation deduced from SAMS species data. *J. Atmos. Sci.*, **45**, 1929-1939.

McIntyre, M. E., 1980: Towards a Lagrangian-mean description of stratospheric circulations and chemical transports. *Phil. Trans. R. Soc. Lond.*, A **296**, 129-148.

Pearson, C. E., 1986: *Numerical Methods in Engineering and Science*. Van Nostrand Reinhold Company Inc., New York, 214pp.

Richtmyer, R. D., and K. W. Morton, 1967: *Difference Methods for Initial-Value Problem* 2nd ed., Interscience Publishers, New York, 405pp.

Roache, P. J., 1972: *Computational Fluid Dynamics*. Hermosa Publishers, 434pp.

Rosenfield, J., E., M. R. Schoeberl, and M. A. Geller, 1987: A computation of the stratospheric diabatic circulation using an accurate radiative transfer model. *J. Atmos. Sci.*, **44**, 859-876.

Rosenlof, K. H., and J. R. Holton, 1993: Estimates of the stratospheric residual circulation using the downward control principle. *J. Geophys. Res*. (in press).

Shine, K., 1989: Sources and sinks of zonal momentum in the middle atmosphere diagnosed using the diabatic circulation. *Quart. J. Roy. Met. Soc.*, **115**, 265-292.

Solomon, S., J. T. Kiehl, R. R. Garcia, and W. Grose, 1986: Tracer transport by the diabatic circulation deduced from satellite observations. *J. Atmos. Sci.*, **43**, 1986, 1603-1617.

Tung, K. K., 1982: On the two-dimensional transport of stratospheric trace gases in isentropic coordinates. *J. Atmos. Sci*., **39**, 2330-2355.

Yang, H., K. K. Tung, E. Olaguer, 1990: Nongeostrophic theory of zonally averaged circulation. Part II: Eliassen-Palm Flux divergence and isentropic mixing coefficient. *J. Atmos. Sci*., **47**, 215-241.

Figure Captions

Fig 1. Zonal mean total heating rates ($K\ day^{-1}$) obtained from the LLNL 2-d model with the eddy heating for the winter solstice condition. The contour interval is 0.5.

Fig. 2. Vertical velocity ($mm\ sec^{-1}$) of the RMMC. The contour interval is 0.5.

Fig. 3. Meridional velocity ($m\ sec^{-1}$) of the RMMC. The contour interval is 0.5.

Fig. 4. Mass flux stream function ($kg\ m^{-1}\ sec^{-1}$) constructed from the RMMC of Figs. 2 and 3.

Fig. 5. Mass flux stream functions ($kg\ m^{-1}\ sec^{-1}$). One integrated from the South pole to North pole in (a), the other one integrated from the North pole to South pole in (b), and the one matched between (a) and (b) in (c). See the description in the text.

Fig. 6. Zonal mean heating rates ($K\ day^{-1}$) from the extended altitude model for winter solstice condition. The contour interval is 1.

Fig. 7. Vertical velocity ($mm\ sec^{-1}$) obtained from the heating in Fig. 6. The contour interval is 2.

Fig. 8. Meridional velocity ($m\ sec^{-1}$) obtained from the heating in Fig. 6. The contour interval is 1.

Fig. 9. Heating rates ($K\ day^{-1}$) constructed by the RMMC in Fig. 7, 8 and temperature through the thermodynamic energy equation. The contour interval is 1.

Fig. 10. Zonal momentum forcing ($m\ sec^{-1}\ month^{-1}$) constructed by the RMMC in Figs. 7, 8 and zonal wind through the zonal momentum equation.

Fig. 11. Stream function ($m^2\ sec^{-1}$) solved from the Equation (11) with the thermal forcing in Fig. 9 and the momentum forcing in Fig. 10.

Fig. 12. Vertical velocity ($mm\ sec^{-1}$) obtained from the stream function in Fig. 11. The contour interval is 2.

Fig. 13. Meridional velocity ($m\ sec^{-1}$) obtained from the stream function in Fig. 11. The contour interval is 1.

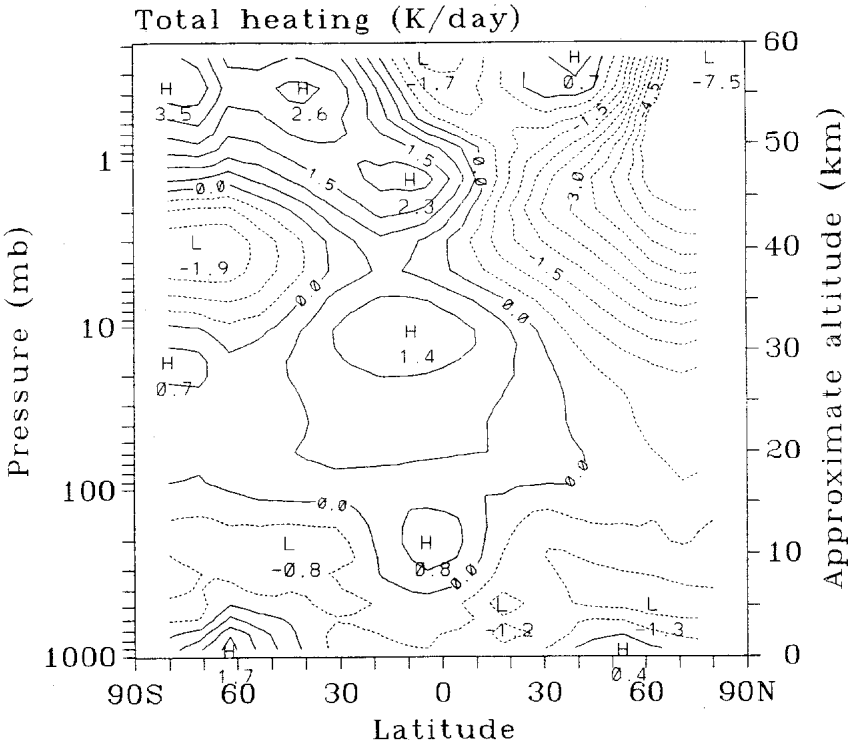

Figure 1

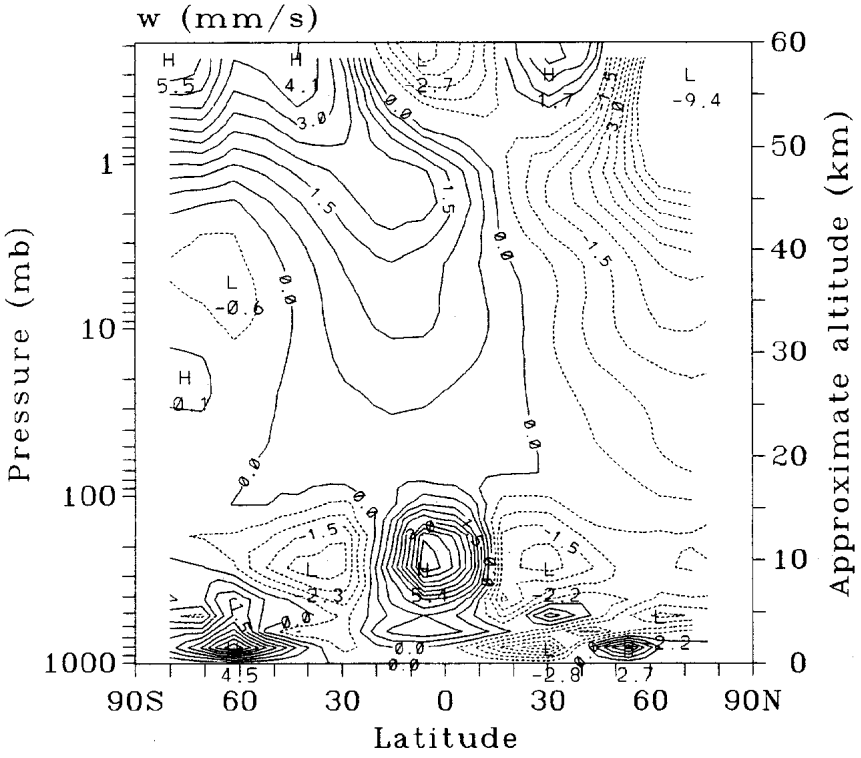

Figure 2

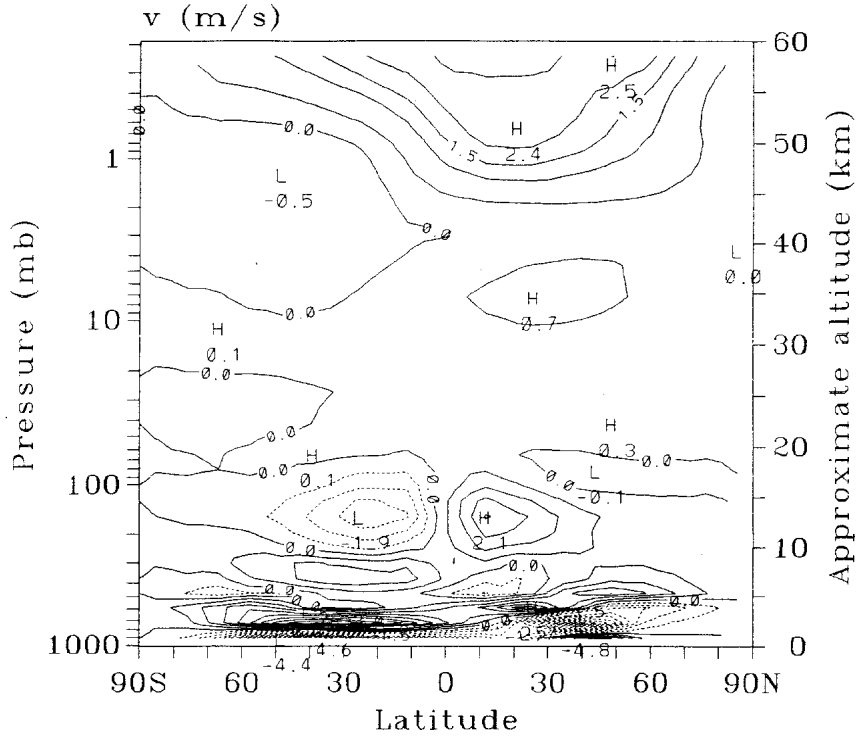

Figure 3

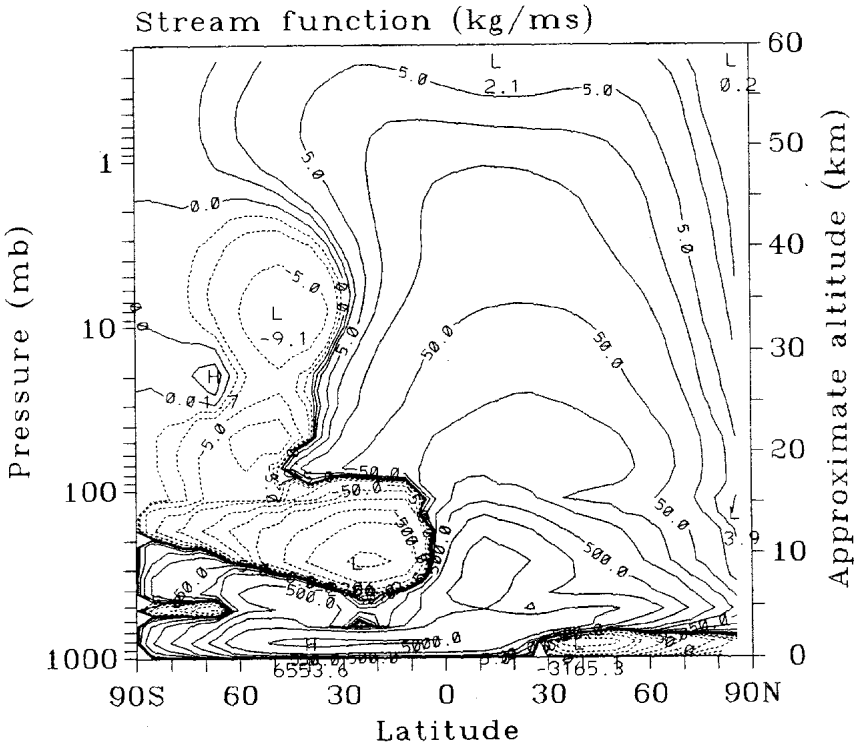

Figure 4

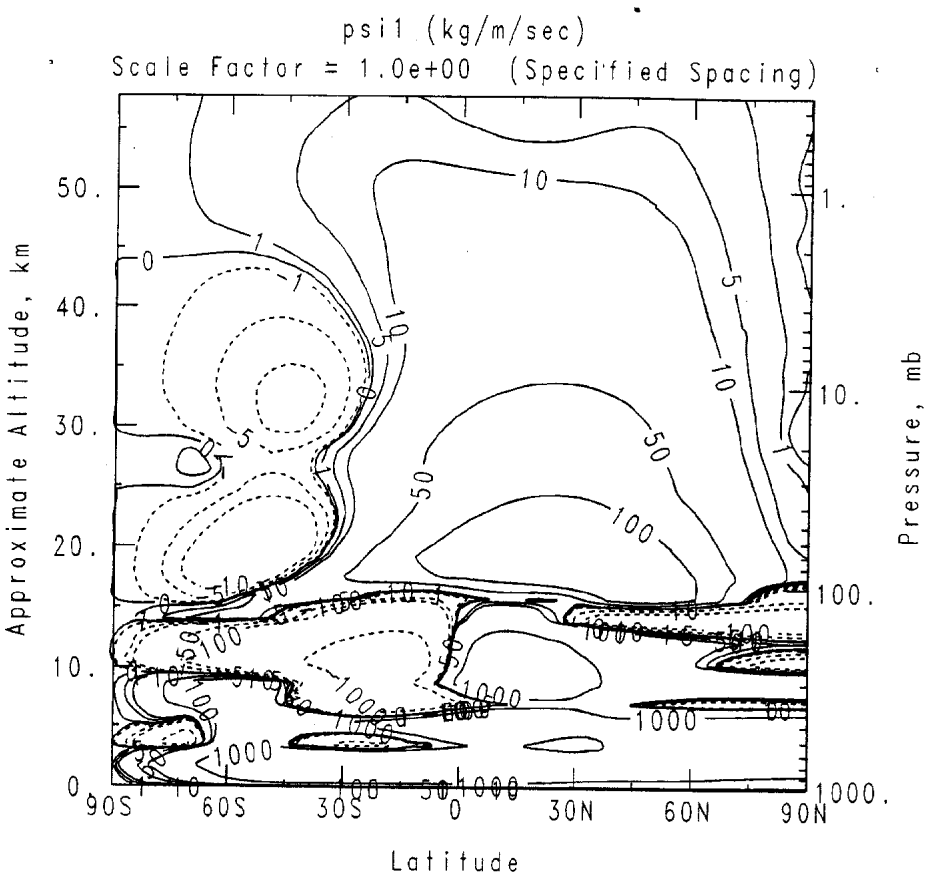
psi1 (kg/m/sec)
Scale Factor = 1.0e+00 (Specified Spacing)
Approximate Altitude, km
50.
40.
30.
20.
10.
0
Pressure, mb
1.
10.
100.
1000.
90S
60S
30S
0
30N
60N
90N
Latitude

Figure 5a

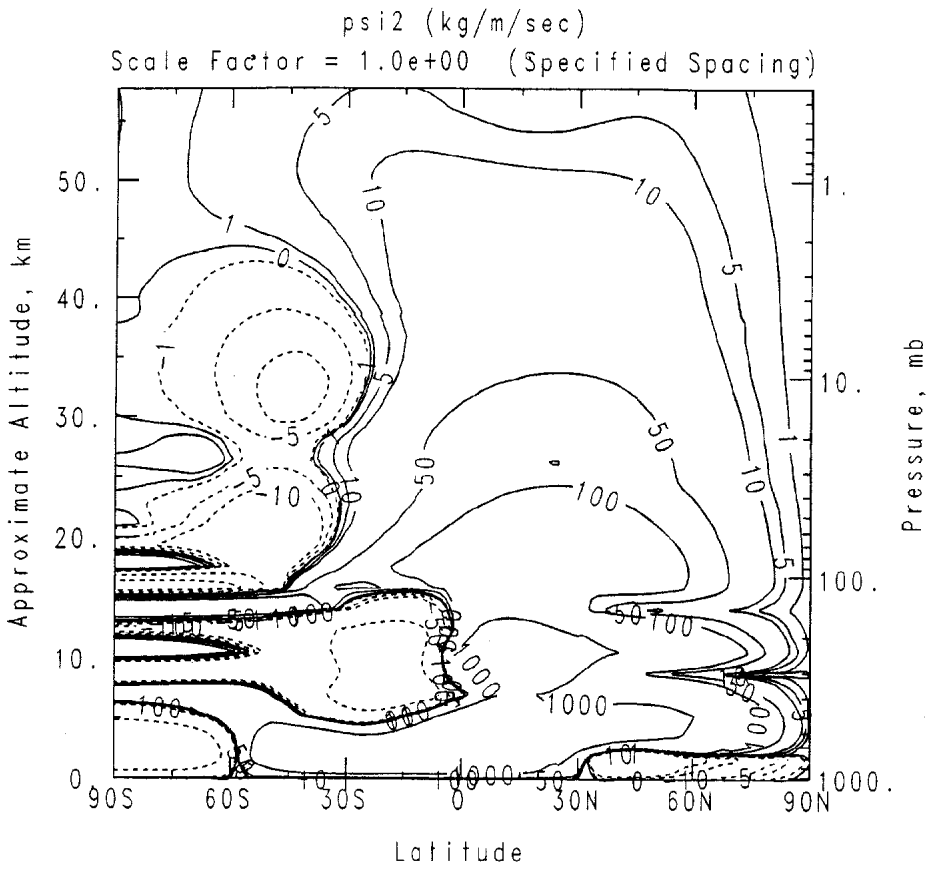
psi2 (kg/m/sec)
Scale Factor = 1.0e+00 (Specified Spacing)
Approximate Altitude, km
50.
40.
30.
20.
10.
0
Pressure, mb
1.
10.
100.
1000.
90S
60S
30S
0
30N
60N
90N
Latitude

Figure 5b

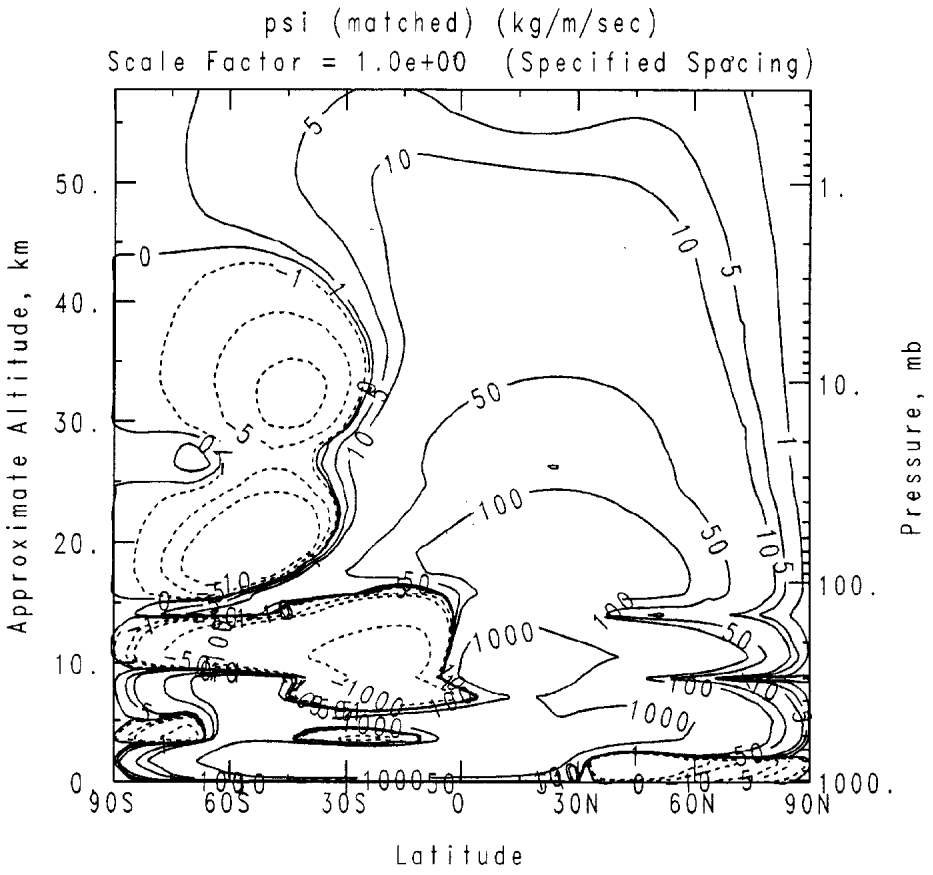
psi (matched) (kg/m/sec)
Scale Factor = 1.0e+00 (Specified Spacing)
Approximate Altitude, km
Pressure, mb
Latitude
90S
60S
30S
0
30N
60N
90N
50.
40.
30.
20.
10.
0
1.
10.
100.
1000.

Figure 5c

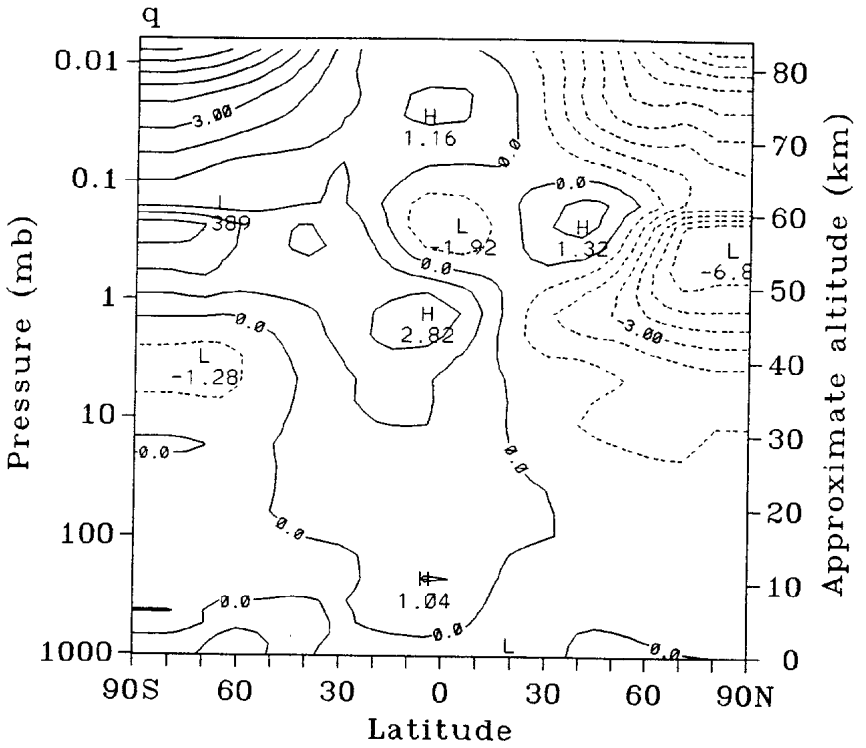

Figure 6

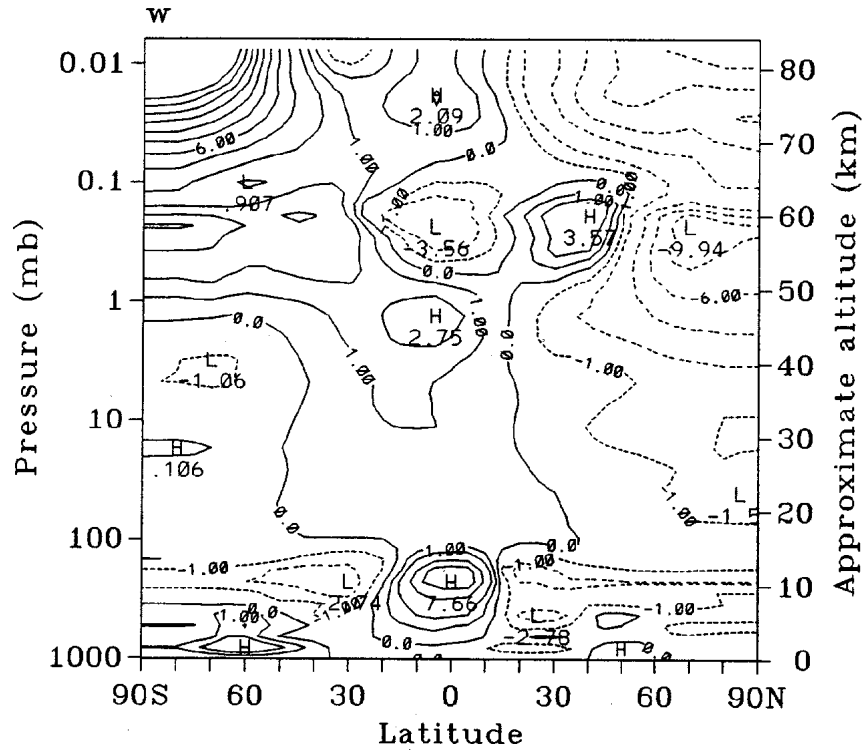

Figure 7

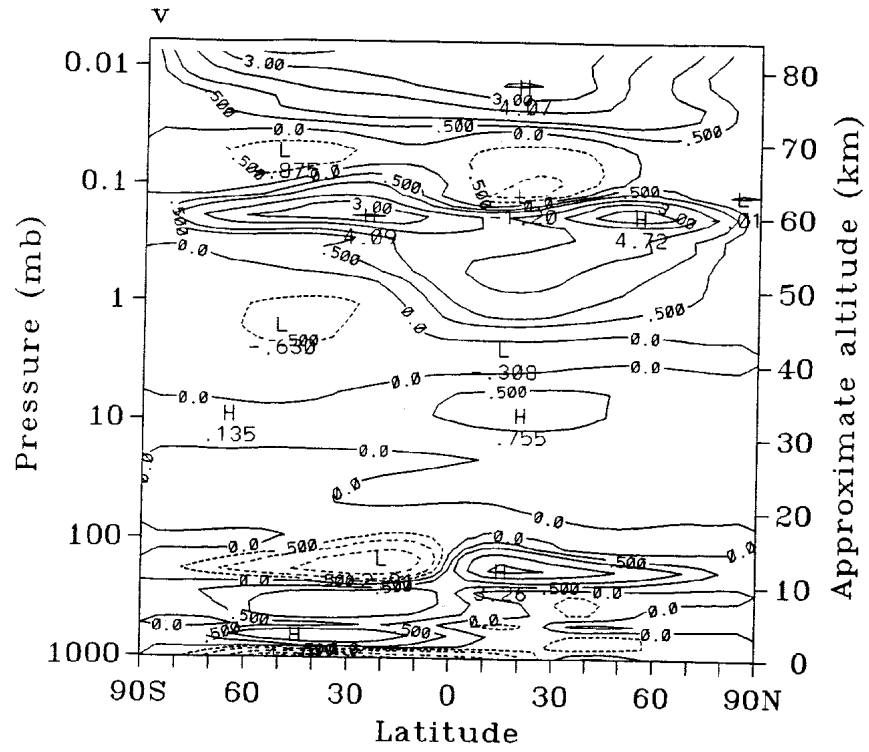

Figure 8

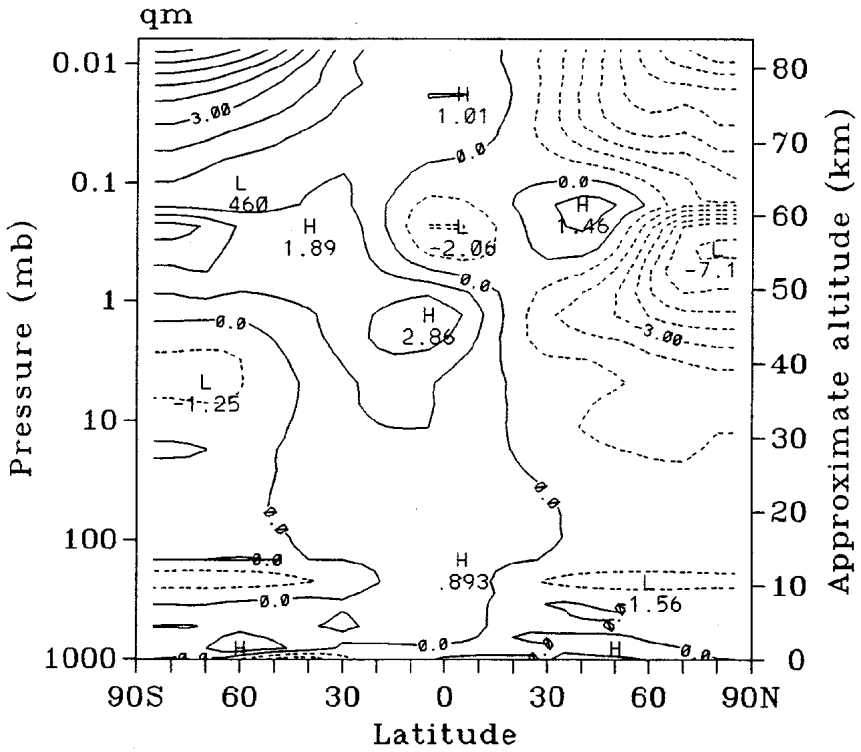

Figure 9

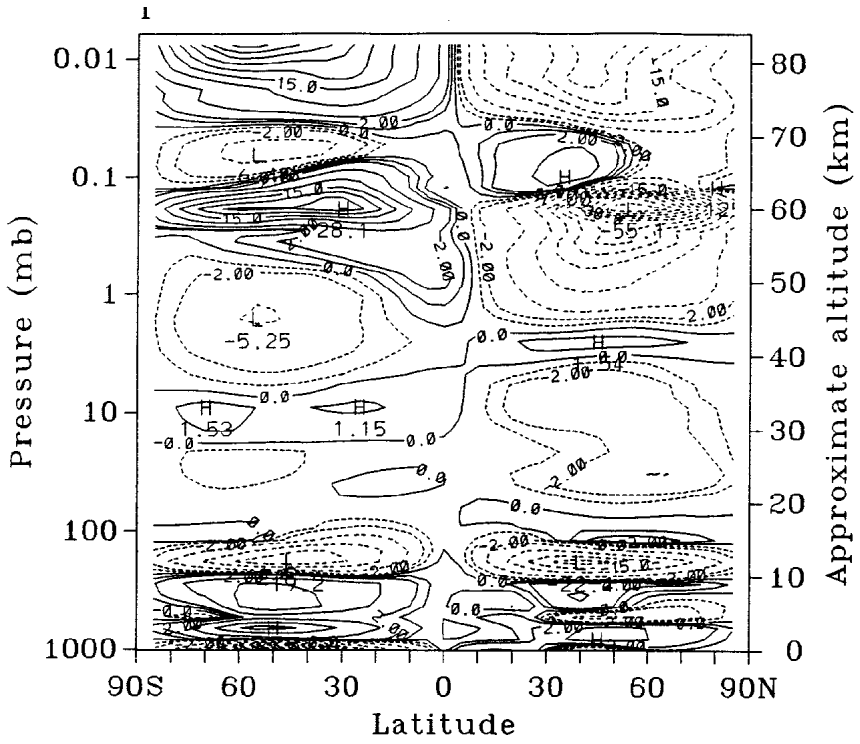

Figure 10

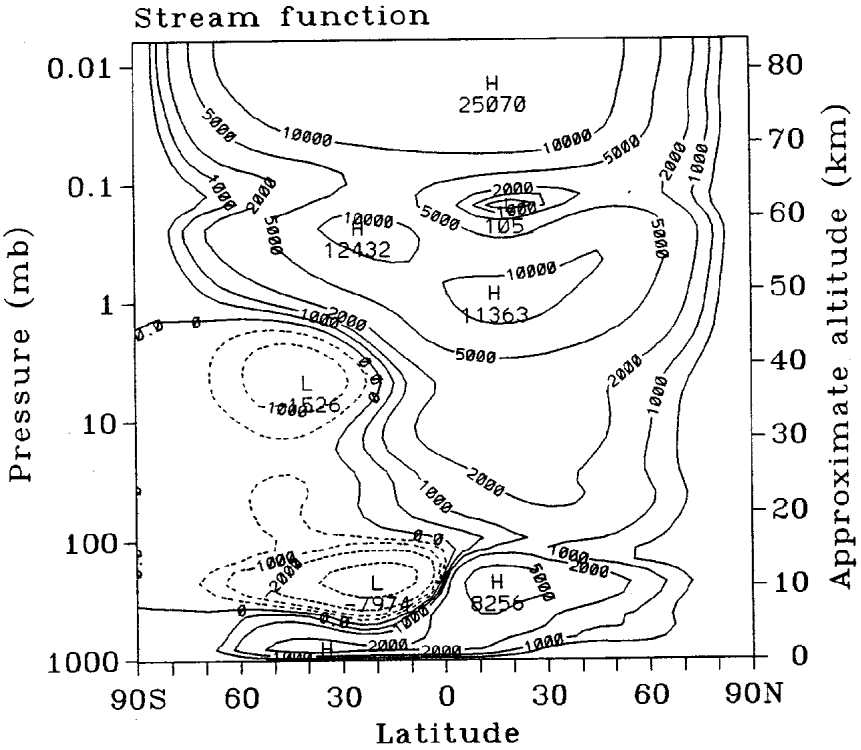

Figure 11

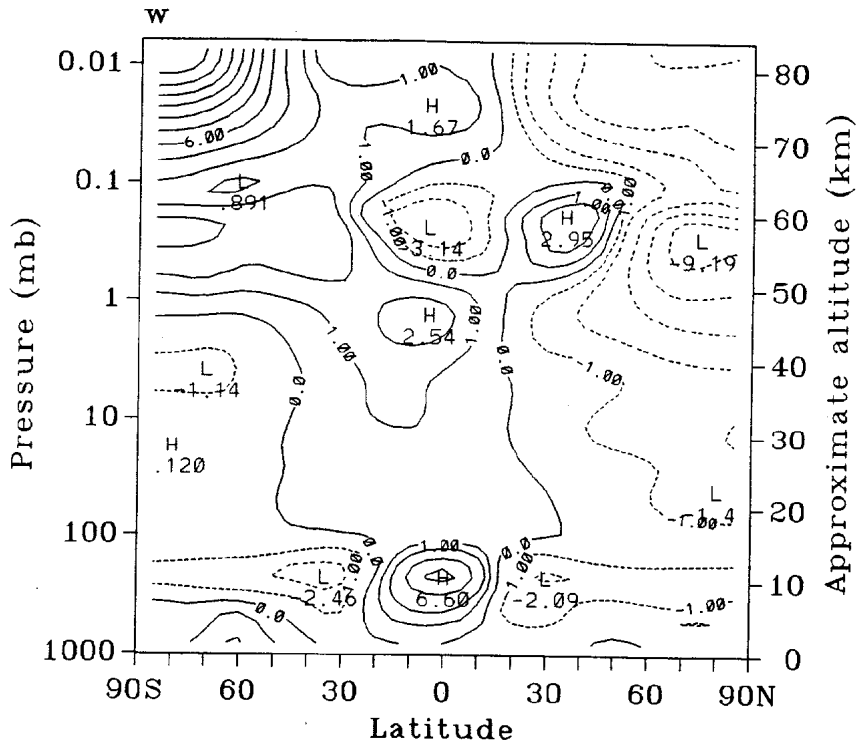

Figure 12

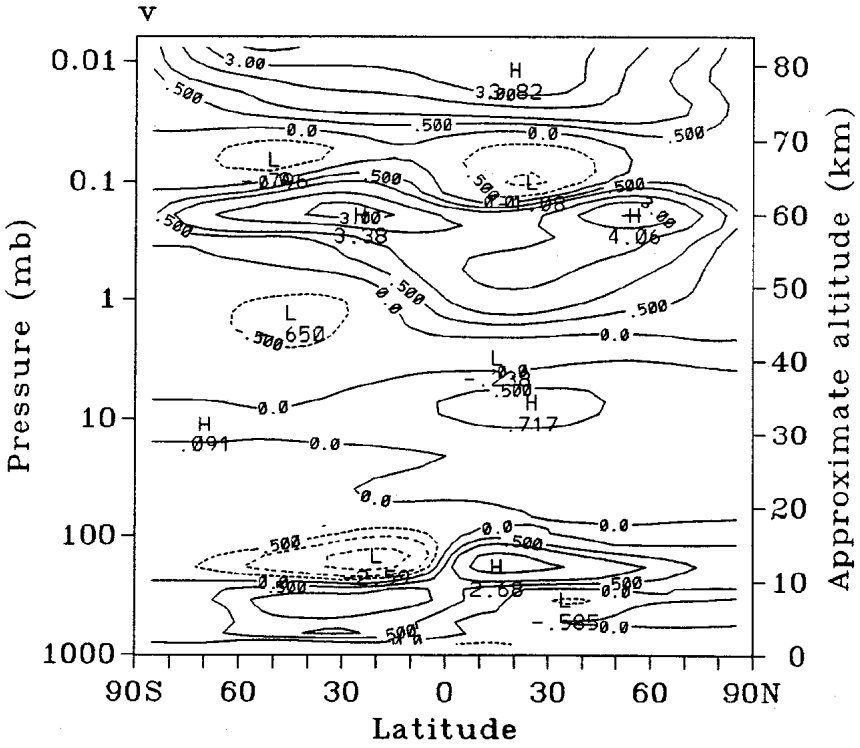

Figure 13

Technical Information Department • **Lawrence Livermore National Laboratory**
University of California • Livermore, California 94551